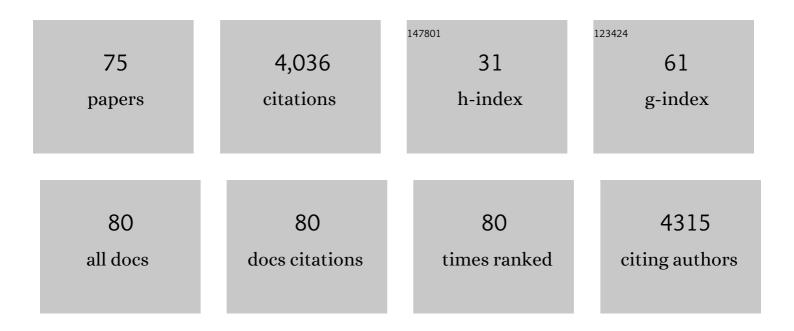
## Qike Jiang

List of Publications by Year in descending order

Source: https://exaly.com/author-pdf/6870477/publications.pdf Version: 2024-02-01



#	Article	IF	CITATIONS
1	Origin of the High Performance in GeTe-Based Thermoelectric Materials upon Bi <sub>2</sub> Te <sub>3</sub> Doping. Journal of the American Chemical Society, 2014, 136, 11412-11419.	13.7	319
2	A 3D Covalent Organic Framework with Exceptionally High Iodine Capture Capability. Chemistry - A European Journal, 2018, 24, 585-589.	3.3	247
3	Enhancing the stability of cobalt spinel oxide towards sustainable oxygen evolution in acid. Nature Catalysis, 2022, 5, 109-118.	34.4	236
4	Exceptional Electrochemical HER Performance with Enhanced Electron Transfer between Ru Nanoparticles and Single Atoms Dispersed on a Carbon Substrate. Angewandte Chemie - International Edition, 2021, 60, 16044-16050.	13.8	200
5	Strong metal-support interaction promoted scalable production of thermally stable single-atom catalysts. Nature Communications, 2020, 11, 1263.	12.8	198
6	Unraveling the High-Activity Origin of Single-Atom Iron Catalysts for Organic Pollutant Oxidation via Peroxymonosulfate Activation. Environmental Science & Technology, 2021, 55, 8318-8328.	10.0	198
7	Potential-Driven Restructuring of Cu Single Atoms to Nanoparticles for Boosting the Electrochemical Reduction of Nitrate to Ammonia. Journal of the American Chemical Society, 2022, 144, 12062-12071.	13.7	192
8	Stable Potential Windows for Longâ€Term Electrocatalysis by Manganese Oxides Under Acidic Conditions. Angewandte Chemie - International Edition, 2019, 58, 5054-5058.	13.8	182
9	Synergistic Effect of Atomically Dispersed Ni–Zn Pair Sites for Enhanced CO <sub>2</sub> Electroreduction. Advanced Materials, 2021, 33, e2102212.	21.0	155
10	Dynamics of Bound Exciton Complexes in CdS Nanobelts. ACS Nano, 2011, 5, 3660-3669.	14.6	132
11	Flexible n-type thermoelectric films based on Cu-doped Bi2Se3 nanoplate and Polyvinylidene Fluoride composite with decoupled Seebeck coefficient and electrical conductivity. Nano Energy, 2015, 18, 306-314.	16.0	119
12	The origin of hematite nanowire growth during the thermal oxidation of iron. Materials Science and Engineering B: Solid-State Materials for Advanced Technology, 2012, 177, 327-336.	3.5	115
13	Layered Bi <sub>2</sub> Se <sub>3</sub> Nanoplate/Polyvinylidene Fluoride Composite Based n-type Thermoelectric Fabrics. ACS Applied Materials & Interfaces, 2015, 7, 7054-7059.	8.0	108
14	Origin of the Activity of Co–N–C Catalysts for Chemoselective Hydrogenation of Nitroarenes. ACS Catalysis, 2021, 11, 3026-3039.	11.2	105
15	A Versatile Approach to Boost Oxygen Reduction of Feâ€N <sub>4</sub> Sites by Controllably Incorporating Sulfur Functionality. Advanced Functional Materials, 2021, 31, 2100833.	14.9	85
16	Fe atoms anchored on defective nitrogen doped hollow carbon spheres as efficient electrocatalysts for oxygen reduction reaction. Nano Research, 2021, 14, 1069-1077.	10.4	71
17	Dramatically enhanced thermoelectric performance of MoS <sub>2</sub> by introducing MoO <sub>2</sub> nanoinclusions. Journal of Materials Chemistry A, 2017, 5, 2004-2011.	10.3	66
18	Photo-thermo semi-hydrogenation of acetylene on Pd1/TiO2 single-atom catalyst. Nature Communications, 2022, 13, 2648.	12.8	61

#	Article	IF	CITATIONS
19	Atomic Insight into the Local Structure and Microenvironment of Isolated Co-Motifs in MFI Zeolite Frameworks for Propane Dehydrogenation. Journal of the American Chemical Society, 2022, 144, 12127-12137.	13.7	60
20	Mesoporous F-doped ZnO prism arrays with significantly enhanced photovoltaic performance for dye-sensitized solar cells. Journal of Power Sources, 2011, 196, 10518-10525.	7.8	54
21	2D Chalcogenide Nanoplate Assemblies for Thermoelectric Applications. Advanced Materials, 2017, 29, 1700070.	21.0	54
22	Creating Edge Sites within the Basal Plane of a MoS <sub>2</sub> Catalyst for Substantially Enhanced Hydrodeoxygenation Activity. ACS Catalysis, 2022, 12, 8-17.	11.2	50
23	Wavy PtCu alloy nanowire networks with abundant surface defects enhanced oxygen reduction reaction. Nano Research, 2019, 12, 2766-2773.	10.4	48
24	High-performance bifunctional oxygen electrocatalyst derived from iron and nickel substituted perfluorosulfonic acid/polytetrafluoroethylene copolymer. Nano Energy, 2016, 30, 801-809.	16.0	46
25	A ZnO/ZnMgO Multiple-Quantum-Well Ultraviolet Random Laser Diode. IEEE Electron Device Letters, 2011, 32, 54-56.	3.9	44
26	Stable Potential Windows for Longâ€Term Electrocatalysis by Manganese Oxides Under Acidic Conditions. Angewandte Chemie, 2019, 131, 5108-5112.	2.0	44
27	Stabilizing the isolated Pt sites on PtGa/Al2O3 catalyst via silica coating layers for propane dehydrogenation at low temperature. Applied Catalysis B: Environmental, 2022, 300, 120731.	20.2	43
28	Enhancement of Mass Transport for Oxygen Reduction Reaction Using Petalâ€Like Porous Feâ€NC Nanosheet. Small, 2021, 17, e2006178.	10.0	42
29	Facile Fabrication of SnO <sub>2</sub> Nanorod Arrays Films as Electron Transporting Layer for Perovskite Solar Cells. Solar Rrl, 2018, 2, 1800133.	5.8	41
30	Enhanced Catalytic Performance through In Situ Encapsulation of Ultrafine Ru Clusters within a High-Aluminum Zeolite. ACS Catalysis, 2022, 12, 1847-1856.	11.2	37
31	Effect of the Configuration of Copper Oxide–Ceria Catalysts in NO Reduction with CO: Superior Performance of a Copper–Ceria Solid Solution. ACS Applied Materials & Interfaces, 2021, 13, 61078-61087.	8.0	37
32	Selfâ€Assembled Heterostructures: Selective Growth of Metallic Nanoparticles on V <sub>2</sub> –VI <sub>3</sub> Nanoplates. Advanced Materials, 2017, 29, 1702968.	21.0	34
33	Exceptional Electrochemical HER Performance with Enhanced Electron Transfer between Ru Nanoparticles and Single Atoms Dispersed on a Carbon Substrate. Angewandte Chemie, 2021, 133, 16180-16186.	2.0	31
34	High performance perovskite solar cells using TiO2 nanospindles as ultrathin mesoporous layer. Journal of Energy Chemistry, 2018, 27, 951-956.	12.9	29
35	Ultraviolet/orange bicolor electroluminescence from an n-ZnO/n-GaN isotype heterojunction light emitting diode. Applied Physics Letters, 2011, 99, 263502.	3.3	28
36	Pd single-atom catalysts derived from strong metal-support interaction for selective hydrogenation of acetylene. Nano Research, 2022, 15, 10037-10043.	10.4	28

#	Article	IF	CITATIONS
37	Promoting oxygen evolution reaction by RuO2 nanoparticles in solid oxide CO2 electrolyzer. Energy Storage Materials, 2018, 13, 207-214.	18.0	27
38	Mesoporous non-noble metal electrocatalyst derived from ZIF-67 and cobalt porphyrin for the oxygen reduction in alkaline solution. Journal of Electroanalytical Chemistry, 2018, 825, 65-72.	3.8	27
39	Modulation of Mo–Fe–C Sites Over Mesoscale Diffusionâ€Enhanced Hollow Subâ€Micro Reactors Toward Boosted Electrochemical Water Oxidation. Advanced Functional Materials, 2022, 32, .	14.9	26
40	Steering the reaction pathway of syngas-to-light olefins with coordination unsaturated sites of ZnGaOx spinel. Nature Communications, 2022, 13, 2742.	12.8	24
41	Efficient Optical Orientation and Slow Spin Relaxation in Lead-Free CsSnBr <sub>3</sub> Perovskite Nanocrystals. ACS Energy Letters, 2021, 6, 1670-1676.	17.4	23
42	Synergizing Surface Hydride Species and Ru Clusters on Sm <sub>2</sub> O <sub>3</sub> for Efficient Ammonia Synthesis. ACS Catalysis, 2022, 12, 2178-2190.	11.2	23
43	The growth of hematite nanobelts and nanowires—tune the shape via oxygen gas pressure. Journal of Materials Research, 2012, 27, 1014-1021.	2.6	22
44	Confined-space synthesis of hierarchical MgAPO-11 molecular sieves with good hydroisomerization performance. Microporous and Mesoporous Materials, 2018, 262, 182-190.	4.4	22
45	Iron stabilized 1/3 A-site deficient La–Ti–O perovskite cathodes for efficient CO <sub>2</sub> electroreduction. Journal of Materials Chemistry A, 2020, 8, 21053-21061.	10.3	22
46	Ultraâ€High Fluorine Enhanced Homogeneous Nucleation of Lithium Metal on Stepped Carbon Nanosheets with Abundant Edge Sites. Advanced Energy Materials, 2022, 12, .	19.5	22
47	Engineering Sensitized Photon Upconversion Efficiency via Nanocrystal Wavefunction and Molecular Geometry. Angewandte Chemie - International Edition, 2020, 59, 17726-17731.	13.8	20
48	Synthesis and characterization of anatase TiO 2 nanosheet arrays on FTO substrate. Journal of Energy Chemistry, 2015, 24, 626-631.	12.9	19
49	Synthesis of Ag/PANI@MnO <sub>2</sub> core–shell nanowires and their capacitance behavior. RSC Advances, 2016, 6, 17415-17422.	3.6	18
50	Bi <sub>2</sub> Te <sub>3</sub> Plates with Single Nanopore: The Formation of Surface Defects and Self-Repair Growth. Chemistry of Materials, 2018, 30, 1965-1970.	6.7	16
51	The bead-like Li3V2(PO4)3/NC nanofibers based on the nanocellulose from waste reed for long-life Li-ion batteries. Carbohydrate Polymers, 2020, 237, 116134.	10.2	16
52	High Performance of Singleâ€atom Catalyst Pd <sub>1</sub> /MgO for Semiâ€hydrogenation of Acetylene to Ethylene in Excess Ethylene. ChemNanoMat, 2021, 7, 526-529.	2.8	14
53	Fe–N–C with Intensified Exposure of Active Sites for Highly Efficient and Stable Direct Methanol Fuel Cells. ACS Applied Materials & Interfaces, 2021, 13, 16279-16288.	8.0	14
54	Ni <sup>2+</sup> â€Directed Anisotropic Growth of PtCu Nested Skeleton Cubes Boosting Electroreduction of Oxygen. Advanced Science, 2022, 9, e2104927.	11.2	14

#	Article	IF	CITATIONS
55	Synthesis of Nickel Nitrideâ€Based 1D/0D Heterostructure via a Morphologyâ€Inherited Nitridation Strategy for Efficient Electrocatalytic Hydrogen Evolution. Small, 2022, 18, .	10.0	13
56	ZnSe Heterocrystalline Junctions Based on Zinc Blendeâ^'Wurtzite Polytypism. Journal of Physical Chemistry C, 2010, 114, 1411-1415.	3.1	12
57	The Mystery from Tetragonal NaVPO <sub>4</sub> F to Monoclinic NaVPO <sub>4</sub> F: Crystal Presentation, Phase Conversion, and Naâ€Storage Kinetics. Advanced Energy Materials, 2021, 11, 2100627.	19.5	11
58	Low-voltage multicolor electroluminescence from all-inorganic carbon dots/Si-heterostructured light-emitting diodes. Journal of Materials Science, 2019, 54, 8492-8503.	3.7	9
59	Targeted killing of tumor cells based on isoelectric point suitable nanoceria-rod with high oxygen vacancies. Journal of Materials Chemistry B, 2022, 10, 1410-1417.	5.8	9
60	Ternary CuCrCeO <sub>x</sub> Solid Solution Enhances N <sub>2</sub> ‧electivity in the NO Reduction with CO in the Presence of Water and Oxygen. ChemCatChem, 2022, 14, .	3.7	9
61	Smallâ€Proteinâ€Stabilized Semiconductor Nanoprobe for Targeted Imaging of Cancer Cells. ChemBioChem, 2016, 17, 1202-1206.	2.6	8
62	Highly efficient electrocatalysts with CoO/CoFe <sub>2</sub> O <sub>4</sub> composites embedded within N-doped porous carbon materials prepared by hard-template method for oxygen reduction reaction. RSC Advances, 2017, 7, 56375-56381.	3.6	8
63	Structural and Optical Characterization of ZnO/Mg <sub><i>x</i></sub> Zn <sub>1–<i>x</i></sub> O Multiple Quantum Wells Based Random Laser Diodes. ACS Applied Materials & Interfaces, 2012, 4, 7043-7046.	8.0	7
64	Nanointerlayer Induced Electroluminescence Transition from Ultraviolet- to Red-Dominant Mode for n-Mn:ZnO/N-GaN Heterojunction. ACS Applied Materials & amp; Interfaces, 2012, 4, 2521-2524.	8.0	7
65	Solution-processed yellow-white light-emitting diodes based on mixed-solvent dispersed luminescent ZnO nanocrystals. Applied Physics Letters, 2015, 106, 263506.	3.3	6
66	Topological doping effects in 2D chalcogenide thermoelectrics. 2D Materials, 2018, 5, 045008.	4.4	5
67	Highly active and stable Ir nanoclusters derived from Ir1/MgAl2O4 single-atom catalysts. Journal of Chemical Physics, 2021, 154, 131105.	3.0	5
68	Effect of twins on the crystallographic characteristics of the Mg17Al12 phase in the pre-compressed AZ91 alloy. Materials Letters, 2018, 230, 166-169.	2.6	4
69	Optimized oxygen reduction activity by tuning shell component in Pd@Pt-based core-shell electrocatalysts. Journal of Colloid and Interface Science, 2021, 604, 301-309.	9.4	4
70	Going Nano with Confined Effects to Construct Pomegranate-like Cathode for High-Energy and High-Power Lithium-Ion Batteries. ACS Applied Materials & Interfaces, 2019, 11, 28934-28942.	8.0	3
71	Transportable Mononuclear Metal Atoms as Building Blocks for Bottomâ€up Material Fabrication: Pt 1 (0) and Au 1 (0) Atoms in Stock Solutions. ChemNanoMat, 2020, 6, 1191-1199.	2.8	3
			_

2D Chalcogenides: 2D Chalcogenide Nanoplate Assemblies for Thermoelectric Applications (Adv.) Tj ETQq0 0 0 rgBT / Overlock 10 Tf 50

#	Article	IF	CITATIONS
73	Selective Hydrogenation of Nitroarenes by Single-Atom Pt Catalyst Through Hydrogen Transfer Reaction. Topics in Catalysis, 2022, 65, 1604-1608.	2.8	2
74	Engineering Sensitized Photon Upconversion Efficiency via Nanocrystal Wavefunction and Molecular Geometry. Angewandte Chemie, 2020, 132, 17879-17884.	2.0	0
75	Singleâ€Atom Catalysts: Enhancement of Mass Transport for Oxygen Reduction Reaction Using Petal‣ike Porous Feâ€NC Nanosheet (Small 6/2021). Small, 2021, 17, 2170024.	10.0	0